Charge and spin transport properties of Mo_2X_2 (X = Fe,Co,Ni) molecular contacts

A. García-Fuente,[1] V. M. García-Suárez,[2,3,4] J. Ferrer,[2,3,4] and A. Vega[1]
[1]*Departamento de Física Teórica, Atómica y Óptica, Universidad de Valladolid, E-47011 Valladolid, Spain*
[2]*Departamento de Física, Universidad de Oviedo, 33007 Oviedo, Spain*
[3]*Nanomaterials and Nanotechnology Research Center, CSIC-Universidad de Oviedo, 33428 Llanera, Spain*
[4]*Department of Physics, Lancaster University, Lancaster LA1 4YB, United Kingdom*
(Received 30 November 2011; published 27 June 2012)

We present a first-principles study of the electronic and transport properties of linear clusters Mo_2X_2 (X = Fe,Co,Ni), formed by two X atoms separated by a nearly nonmagnetic Mo dimer, connected to gold electrodes. Density functional theory, as implemented in the SIESTA code with the generalized gradient approximation, is used to determine the spin-polarized electronic structure of the molecular contact for relaxed distances. We show that the Mo_2X_2 clusters anchored to the gold electrodes have two different magnetic states, corresponding to the spin isomers found in the freestanding environment, one of which has parallel magnetic coupling between the X atoms across the Mo dimer and another that has antiparallel coupling. The transmission coefficients, current-voltage characteristics, and conductivity are then computed with the SMEAGOL code for the two magnetic states. We show that this system presents spin-filtering properties and magnetoresistance driven by the magnetic state of the molecular contact.

DOI: 10.1103/PhysRevB.85.224433 PACS number(s): 73.63.−b, 72.60.+g, 31.15.A−, 73.23.Ad

I. INTRODUCTION

The field of molecular electronics has become in the last decade a hot topic in physics and materials science. Quantum phenomena occurring at the nanoscale are critical in properties related to the electronic structure of the system. The electronic transport across a molecular system connecting source and drain electrodes is a prototypical example of such properties. The energy spectrum of the molecule is quantized, which means that complex behavior of the electronic current when the molecule or cluster is attached to metallic electrodes may arise. Understanding how the contact affects the electronic structure of the scattering region and what is the behavior of the system subject to a finite voltage bias are questions of fundamental interest. The nature of the electrodes plays also an important role, because it determines the structural properties of the contact, the asymptotic conduction channels, and their alignment with the molecular orbital energy levels.[1] The wide variety of phenomena that are found can be exploited to improve known electrical or magnetoresistive functionalities or to invent new ones.

Remarkable progress in the experimental growth, control, and characterization techniques at the nanoscale has allowed to produce prototype devices such as conducting wires, point contacts, and switches.[2] Single molecular switches[3] have already been studied, both experimentally[4,5] and theoretically. Joachim and Gimzewski[4] proved that the conductance of a fullerene molecule (C_{60}) dramatically changes when it is deformed by a scanning tunneling microscope (STM) tip. Piva *et al.*[5] demonstrated that the current that flows through a molecule on a surface strongly depends on the charge state of nearby surface atoms. Other groups measured similar switching behaviors produced by changes generated by the bias voltage[6,7] or spontaneously.[8] More recent experiments studied the switching produced by conformal changes due to the rotation of molecular rings.[9,10] On the theoretical side there have been already many proposals of molecular switches. We can cite, e.g., Emberly and Kirczenow, who predicted the smallest molecular switch based on a benzene dithiolate molecule between gold leads;[11] Kim *et al.*,[12] who studied switching behavior in complex molecules; and Liu *et al.*, who proposed a spin-based molecular switch.[13] This last example is particularly interesting and relevant for our study because it shows that nanoscale switches could be achieved by using magnetic elements.

Molecular magnets are of particular interest due to the spin dependence of the electronic transport properties.[14–17] Recent systematic *ab initio* calculations of the freestanding binary $Mo_{4-x}Fe_x$ clusters in the whole range of concentrations have shown that certain isomers can be good candidates for molecular electronic devices.[18] In particular, it has been shown that the stable linear isomer of Mo_2Fe_2 is formed by two Fe atoms separated by a nearly nonmagnetic Mo dimer. The formation of tightly bonded dimers of Mo is a common feature of these binary clusters as well as of pure Mo clusters,[19] and it is a consequence of the exact Mo band half filling, which results in a strong covalent bond with paired electrons. This linear homotope of Mo_2Fe_2 has two spin isomers which differ in the magnetic coupling between the two external Fe atoms. The atomic spins of the two Fe atoms are aligned parallel in one of the two isomers and antiparallel in the other, therefore showing either ferromagnetic (FM) or antiferromagnetic (AFM) behavior, respectively. The lowest-energy isomer corresponds to the AFM coupling, similar to what was observed recently in [Fe (1.5 nm)/Mo (t nm)] multilayers prepared by electron-beam evaporation.[20] These clusters can be viewed as the one-dimensional atomic limit of the FM- and AFM-coupled sandwiches and multilayers to which magnetoresistance effects have been directly related.[21,22] Therefore, a calculation of their transport properties when contacted by metallic electrodes is indeed timely. Interesting effects based on the spin degree of freedom are expected to appear, such as magnetoresistance, spin filtering, and switching behavior. A similar switching behavior using organic dicobaltocene molecules was predicted some time ago.[13]

Many recent numerical developments in the theory of quantum transport are based on the Keldysh-Kadanoff-Baym nonequilibrium Green's function (NEGF) formalism.[23] The SMEAGOL code[24,25] is a flexible and efficient implementation of this formalism. SMEAGOL obtains the Hamiltonian from the density functional theory (DFT)[26] code SIESTA,[27] which uses pseudopotentials and a localized basis set of pseudoatomic orbitals and calculates self-consistently the density matrix, the transmission, and the current for each bias voltage.

We employed SMEAGOL in the present work to simulate a source and a sink of gold electrodes connected through the Mo_2X_2 cluster and to study the electronic transport properties across this molecular magnet. We first calculate with SIESTA the electronic structure of the contact with relaxed distances. The transmission coefficients and $I-V$ characteristics are then calculated for spin-dependent electronic currents passing through the scattering region produced by the molecular magnet in its two possible magnetic states. We show that this system presents spin-filtering properties, magnetoresistance, and switching behavior depending on the magnetic state of the molecular contact.

We give the details of our DFT calculations in the next section. We present and discuss the structural properties of the nanostructure in Sec. III. Our results for the nanostructure transport results are given in Sec. IV. The main conclusions are summarized at the end.

II. DETAILS OF THE DFT APPROACH

We have done calculations of the electronic and structural properties of these systems with the DFT code SIESTA.[27] This method employs a linear combination of pseudoatomic orbitals for the basis set and replaces the atomic cores by nonlocal norm-conserving Troullier-Martins pseudopotentials,[28] factorized in the Kleinman-Bylander form.[29] In our calculation, the exchange-correlation potential was calculated with the generalized gradient approximation (GGA) as parametrized by Perdew, Burke, and Ernzerhof.[30,31] The pseudopotentials of Fe, Co, and Ni were generated with an atomic configuration of $3d^7\ 4s^1$, $3d^8\ 4s^1$, and $3d^9\ 4s^1$, respectively. The Mo pseudopotential was generated with a $4d^5\ 5s^1$ atomic configuration. We included nonlinear core corrections to account for the significant overlap of the semicore and the valence states. A double-ζ polarized (DZP) basis set is used as the basis set in all these cases.

For the relaxation of the system connected to Au electrodes we used a basis set for Au that included the filled $5d$ states and the $6s$ and the empty $6p$ states, which interact with the Mo_2X_2 molecule and affect the bonding between the molecule and the surface. We carried out the transport calculations with a simpler basis containing only the $6s$ pseudo-orbitals, because these are the orbitals which determine the conduction channels at the leads and are mainly responsible for the transmission at the Fermi level. This description is accurate enough, as the $5d$ ($6p$) states in Au bulk are well below (above) the Fermi level and do not affect to the transport properties; i.e., we know from calculations of other molecular systems that the inclusion of only the gold $6s$ states produces a very similar transmission from -2 eV below the Fermi energy to energies just below the lowest unoccupied molecular orbital (LUMO) in case of molecules coupled on a pyramidal configuration to the gold surface (see below). The transmission at the Fermi level can be a bit overestimated, however, which would give rise to bigger currents, but the overall qualitative shape of the $I-V$ curves should be very similar.

The transport calculations have been performed using the SMEAGOL program,[24] whereby the system is split into three parts: left and right leads (L and R, respectively), and a scattering region (M), which includes the molecule and those pieces of the leads that are modified by the presence of the molecule and the surfaces. At the Hamiltonian level this system is described by an infinite Hermitian matrix $\mathcal{H}$. This, however, has a rather regular structure. First notice that the two semi-infinite leads are assumed to be defect-free crystalline metals. These have a regular periodic structure and a unit cell along which the direction of the transport can be defined. Notice that the Hamiltonian matrix is rather sparse because of the localized atomic orbital basis set used in SIESTA. We then classify all atoms in the leads in terms of principal layers (PLs). A principal layer is the smallest cell that repeats periodically in the direction of the transport constructed so that it interacts only with the nearest-neighbor PLs. This means that *all* the matrix elements between atoms belonging to two nonadjacent PLs vanish. H_0 is defined as the $N \times N$ matrix describing all interactions within a PL, where N is the total number of degrees of freedom (basis functions) in the PL [note that we use calligraphic symbols ($\mathcal{H}$) for infinitely dimensional matrices and capital italic letters (H) for finite matrices]. Similarly H_1 is the $N \times N$ matrix describing the interaction between two PLs. Finally H_{M} is the $M \times M$ matrix describing the extended molecule and H_{LM} (H_{RM}) is the $N \times M$ matrix containing the interaction between the last PL of the left-hand side (right-hand side) lead and the extended molecule. The final form of $\mathcal{H}$ is

$$\mathcal{H} = \begin{pmatrix} . & . & . & . & . & . & . & . & . & . & \\ . & 0 & H_{-1} & H_0 & H_1 & 0 & . & . & . & . & . \\ . & . & 0 & H_{-1} & H_0 & H_{\mathrm{LM}} & 0 & . & . & . & . \\ . & . & . & 0 & H_{\mathrm{ML}} & H_{\mathrm{M}} & H_{\mathrm{MR}} & 0 & . & . & . \\ . & . & . & . & 0 & H_{\mathrm{RM}} & H_0 & H_1 & 0 & . & . \\ . & . & . & . & . & 0 & H_{-1} & H_0 & H_1 & 0 & . \\ . & . & . & . & . & . & . & . & . & . & . \\ & & & & & & & & & & \end{pmatrix}. \tag{1}$$

For a system which preserves time-reversal symmetry, $H_{-1} = H_1^\dagger$, $H_{\rm ML} = H_{\rm LM}^\dagger$, and $H_{\rm MR} = H_{\rm RM}^\dagger$. The overlap matrix $\mathcal{S}$ has exactly the same structure as $\mathcal{H}$. Therefore, we adopt the notation S_0, S_1, $S_{\rm LM}$, $S_{\rm RM}$, and $S_{\rm M}$ for the various blocks of $\mathcal{S}$, in complete analogy with their Hamiltonian counterparts. Here the principal layer, defined by $\mathcal{H}$, is used for both the $\mathcal{S}$ and the $\mathcal{H}$ matrices, even though the range of $\mathcal{S}$ can be considerably shorter than that of $\mathcal{H}$.

Using the above Hamiltonians, we can compute the retarded *surface* Green's function of the unconnected leads $G_{\rm L}^{0\rm R}$ and $G_{\rm R}^{0\rm R}$. These are used to compute the retarded self-energies for the left- and right-hand-side leads

$$\Sigma_{\rm L}^{\rm R}(E) = (\epsilon^+ S_{\rm ML} - H_{\rm ML}) G_{\rm L}^{0\rm R}(E) \, (\epsilon^+ S_{\rm LM} - H_{\rm LM}) \tag{2}$$

and

$$\Sigma_{\rm R}^{\rm R}(E) = (\epsilon^+ S_{\rm MR} - H_{\rm MR}) G_{\rm R}^{0\rm R}(E) \, (\epsilon^+ S_{\rm RM} - H_{\rm RM}) \, . \tag{3}$$

Using the above quantities, SMEAGOL computes the spin-dependent current using the Landauer formula[23]

$$I_\sigma(V) = \frac{e}{h} \int dE \; T_\sigma(E,V) \; (f(E-\mu_L) - f(E-\mu_R)) \tag{4}$$

where $T_\sigma(E,V)$ are the spin-, energy- and voltage-dependent transmission coefficients of the junction, and whose chemical potentials $\mu_{\rm L/R} = \mu \pm eV/2$ are the equilibrium chemical potential shifted by the voltage bias V. The transmission coefficients are computed using the nonequilibrium Green's function formalism[24] and are given by (the spin-index is omitted hereafter for simplicity)

$$T(E,V) = {\rm Tr}[\, \Gamma_{\rm L}(E - eV/2) \, G_{\rm M}^{\rm R\dagger}(E) \, \Gamma_{\rm R}(e + eV/2) \, G_{\rm M}^{\rm R}(E)], \tag{5}$$

where $G_{\rm M}^{\rm R}(E)$ is the retarded Green's function of the molecule and

$$\Gamma_{\rm R/L}(E) = i \left[\, \Sigma_{\rm L/R}^{\rm R}(E) - \Sigma_{\rm L/R}^{\rm R}(E)^\dagger \right] \tag{6}$$

are the electrode's linewidths, that are computed from the electrode's self-energies.[24]

III. STRUCTURAL PROPERTIES

In a previous work, we studied the structural and electronic properties of freestanding $Mo_{4-x}Fe_x$ structures.[18] We found that the Mo_2Fe_2 ground state consists of a linear structure with a tightly bound Mo dimer separating the Fe atoms. The iron magnetic moments are saturated to a value of $3.2\mu_{\rm B}$ and have an AFM coupling. This structure has a spin isomer with the magnetic moments of the Fe atoms coupled ferromagnetically, which is only 10 meV higher in energy, while the closest stable structure lies more than 0.1 eV higher in energy. This linear system can be seen as the atomic limit of interlayer exchange coupling (IEC) systems made of magnetic sandwiches and multilayers. Therefore, interesting magnetoresistive effects are expected to appear at low temperatures.

We present in this section the dependence of the structural properties of Mo_2X_2, with X = Fe,Co,Ni on the magnetic element X. The main results are shown in Fig. 1, where the three most stable structures of Mo_2X_2 are displayed, together

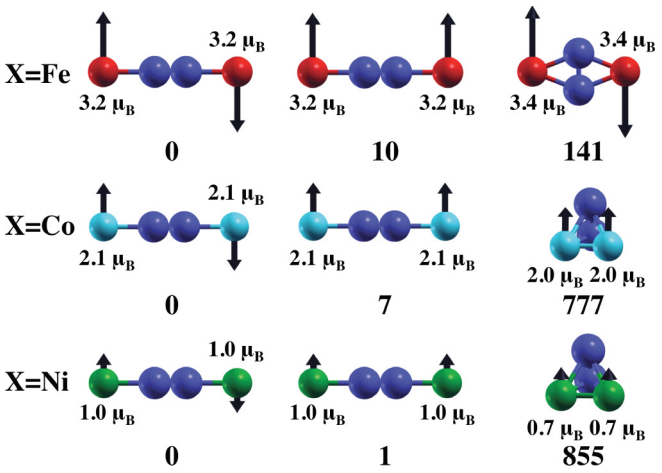

FIG. 1. (Color online) Most stable structures of the system Mo_2X_2 with X = Fe,Co,Ni. We show the magnetic moments on each X atom to distinguish between different spin-isomers. The magnetic moments of Mo are small and not distinguishable in the figure. Energy differences respect to the ground state are shown, in meV, below each structure.

with their energy relative to the ground state. The figure also shows the magnetic moment of each X atom. The Mo magnetic moments are much smaller, of the order of $0.1\mu_{\rm B}$, and are not distinguishable in the figure. The most stable structure is linear-like and has a Mo dimer separating two X atoms with saturated magnetic moments coupled antiferromagnetically for the three transition-metal elements. A FM isomer appears close in energy in all cases. The energy difference between spin isomers decreases from 10 to 1 meV as we move from X = Fe to X = Ni, following the same trend as the magnetic moment. In all the linear structures, the small magnetic moment of each Mo atom has an AFM coupling with the nearest X atom, so that the isolated structures present a quantized total magnetic moment. Also, in all cases the next structurally different isomer lies several hundred meV higher in energy. We therefore believe that these linear Mo_2X_2 (X = Fe,Co,Ni) nanostructures can be realized and characterized experimentally at low temperatures, while the two- or three-dimensional isomers should be suppressed.

We have attached the linear nanostructures to semi-infinite (100) Au electrodes to determine their transport properties. We have relaxed the surface and cluster atomic positions, as well as the distance between the electrodes. We have found that the atomic distortion at the Au surface is negligible for the most stable configuration. We tested three different coupling configurations where the X atoms were placed at pyramidal, bridge, and top positions of both Au surfaces, having coordination numbers of 4, 2, and 1, respectively. We have found that the pyramidal configuration is always the most stable by several eV. Other configurations that involve adatoms due to surface roughness or that depart from a perpendicular configuration due to temperature fluctuations[32] cannot be strictly ruled out.[33] This configuration corresponds, however, to the most probable case, that which gives the peak value in the conductance histogram. The ground state of the system based on the Mo_2Fe_2 molecule is shown in Fig. 2 and the most relevant information is given in Table I. In this table we also

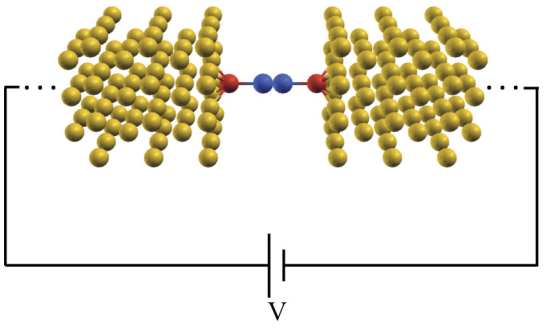

FIG. 2. (Color online) Structure of the complete system made of a Mo_2Fe_2 linear system anchored to two Au surfaces in the (001) direction, which act as electrodes.

show the electronic charge transfer from the molecule to the Au leads, determined from a Mulliken analysis. This charge transfer induces an increase in the magnetic moment of Fe and Co; meanwhile, the opposite occurs for Ni. We have found that the distances between atom X and the Mo slightly increase with respect to the isolated case due to the binding with the Au electrode, while the length of the dimer remains almost constant. We define the binding energy of the molecule with each surface (E_B) as the negative of the difference between the energies of the complete system and of the isolated clusters and Au surfaces, divided by 2. The positive sign of these binding energies shows that the formation of the nanobridge is clearly exothermic in all the cases.

We plot in Fig. 3 the density of states (DOS) of each structure projected on each atom for the isolated-clusters case and compare it to the case where the molecule is anchored to Au electrodes to study the effect of hybridization with the leads. In the isolated case, Fe- and Co-based systems present a clear gap between occupied and unoccupied states, which is the same for both spin components in AFM systems and much larger for the spin-up component than for spin-down due to magnetic saturation in the FM systems. In Ni-based systems, the gap about the Fermi level is much smaller in both AFM and FM cases for the spin-down component, which is a consequence of the presence of more states associated to the transition metal at the Fermi level. When the molecules are connected to the Au electrodes, hybridization with the Au states produces a widening of the peaks of the DOS as a consequence of the electronic delocalization. In this case all the gaps disappear. Different electronic and transport properties are expected for each system depending on which states are present around the Fermi level.

TABLE I. Information of interest about the structure and stability of the Mo_2X_2 molecule connected to Au electrodes. The values of d_{Au-X}, d_{X-Mo}, and d_{Mo-Mo} are measured in Å and refer to the distance between an X atom and the Au surface, a Mo atom and an X atom, and the two Mo atoms, respectively. E_B is the binding energy of the Mo_2X_2 molecule with each Au surface measured in eV. Δq is the change in the charge of the molecule with respect to the isolated case, in units of the electron charge. m_X is the magnetic moment localized on each atom X in Bohr magnetons.

Element (X)	d_{Au-X}	d_{X-Mo}	d_{Mo-Mo}	E_B	Δq	m_X
Fe	1.48	2.73	1.58	3.84	−0.63	3.5
Co	1.48	2.67	1.58	3.61	−0.54	2.3
Ni	1.49	2.63	1.60	3.87	−0.55	0.7

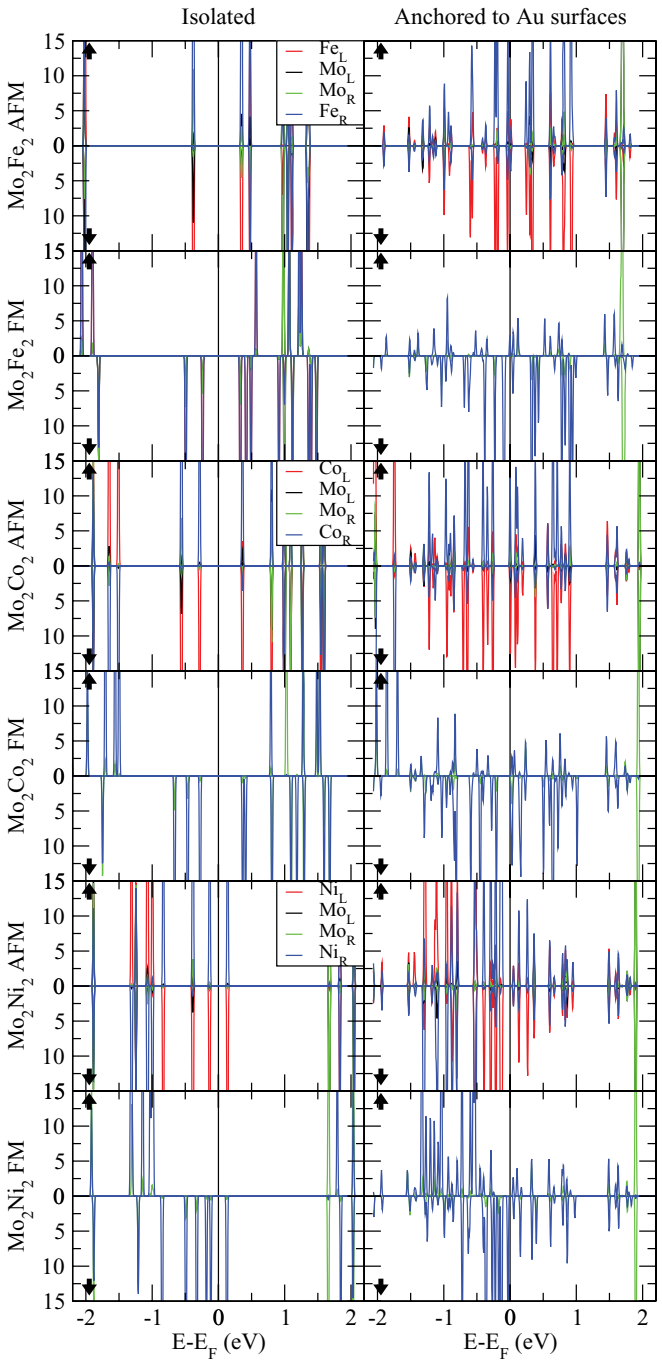

FIG. 3. (Color online) Density of states projected on each atom for the AFM and the FM spin isomers of the Mo_2X_2 linear system, with X = Fe,Co,Ni, in the isolated case compared to the case where the system is anchored to the Au surfaces. The subindex of the atoms refers to their position, where L and R correspond to the left and the right part of the molecule. Notice that in the FM molecules the density of states on X_L and Mo_L are opposite to the ones on X_R and Mo_R. Only the latter are shown in the figure.

IV. TRANSPORT PROPERTIES

We plot in Fig. 4 the transmission coefficients at different voltage biases for the three nanobridge constrictions. At zero bias the AFM configurations are spin symmetric and the transmission coefficients are the same for spin-up and spin-down components. The junctions have a transmission channel for each spin and the total transmission drops at about the Fermi level for Fe, around 0.3 eV for Co, and at −0.2 eV for Ni. However, the FM configurations present nearly one full transmission channel around the Fermi level for the spin-up component, mainly due to *sp* delocalized electrons, while for the spin-down component the more localized *d* states produce more erratic transmission curves (Fig. 3). Of special interest is the case of Fe, where the transmission around the Fermi level nearly drops to zero, so strong spin-filtering effects can be expected. This system would be especially interesting for spintronic applications. To further clarify the electronic and transport properties of this case we plot in Fig. 5 the real-space projection of the density of states around the Fermi level for both spin components with AFM and FM configurations. The AFM configuration shows charge densities for each spin component which are symmetric with each other, with the charge mainly localized around one of the Fe atoms and its nearest Mo atom. The FM configuration shows for the spin-up component a much more delocalized charge density through the junction, which explains the large value of the transmission at the Fermi level. For the spin-down component, however, the charge is more localized on the Fe atoms and it disappears towards the Mo dimer, which explains why the transmission falls in this case (Fig. 4).

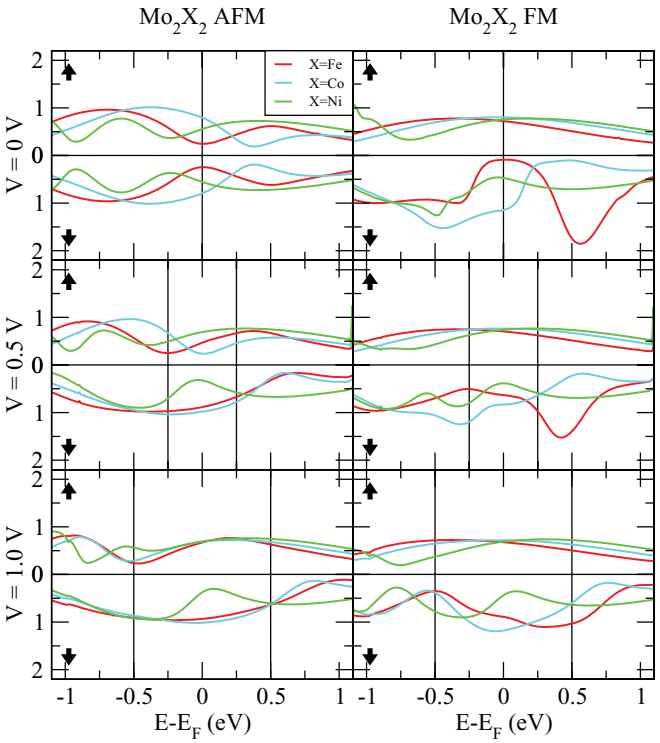

FIG. 4. (Color online) Transmission coefficients for a Mo_2X_2 molecule between Au electrodes, shown for different bias voltages V from 0 to 1 V. Red, blue, and green lines correspond to $X =$ Fe, Co, and Ni, respectively.

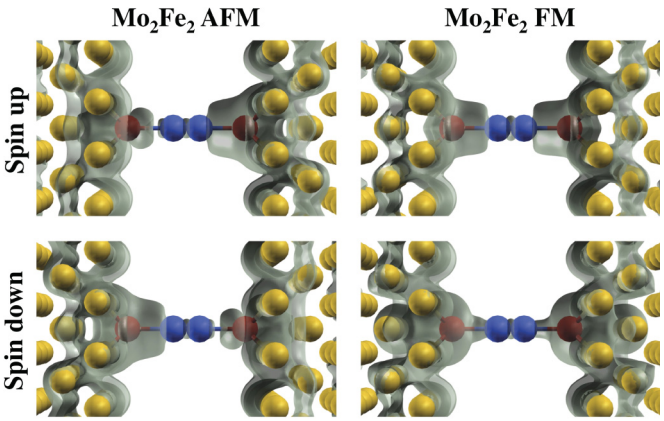

FIG. 5. (Color online) Spatial density of charge around the Fermi level for both spin components of the Mo_2Fe_2 linear system between Au electrodes in the AFM and FM configurations.

We have also computed the current through these systems in a bias window from 0 to 1 V. The results are shown in Fig. 6. The AFM nanobridges yield the same current for spins up and down at low bias due to the symmetry of the system. However, when the bias is larger than 0.1 V, the symmetry is lost and both spin currents start to differ. Around the Fermi level, the spin-up states, which are more localized at the right-hand part of the molecule (see Fig. 5) and are close to the right-hand (positive) electrode, decrease their energy under a positive bias and the transmission curve (Fig. 4) moves gradually to lower energies. The opposite happens for the spin-down component. Notice that the current through the system is proportional to the integral of the transmission coefficients in the energy window $(E_F - eV/2, E_F + eV/2)$, which is also shown Fig. 4. The spin-down current is always larger than the spin-up current for $X =$ Fe,Co, while in the case of Ni the spin-up current is slightly higher.

In the FM systems the two spin components of the transmission are already different at zero bias, so different

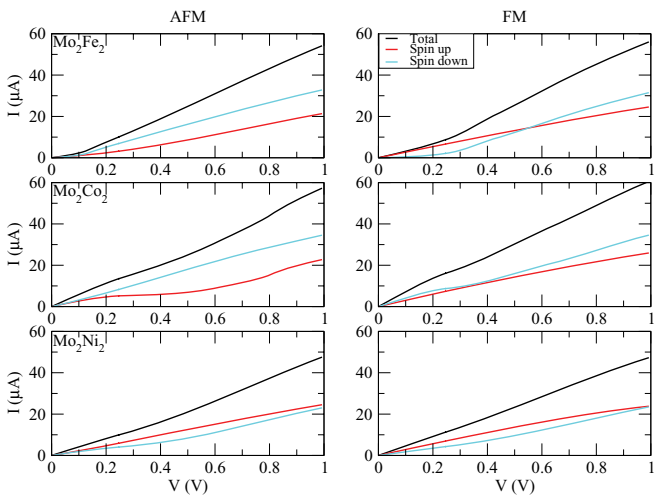

FIG. 6. (Color online) $I-V$ characteristics for a Mo_2X_2 molecule with AFM and FM configurations between Au electrodes.

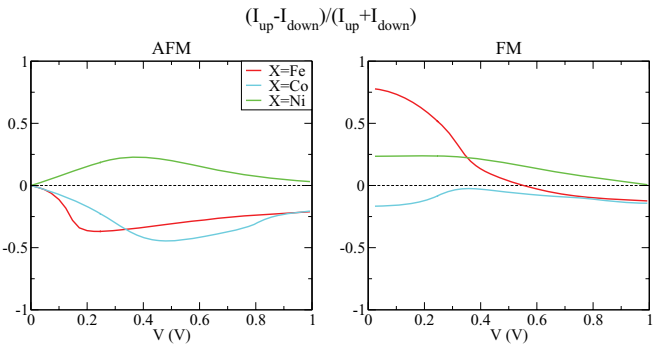

FIG. 7. (Color online) The spin-filtering properties of the different Mo_2X_2 molecules between Au electrodes, estimated in terms of the normalized spin current ΔI.

currents for each spin are found even for V close to 0. In the case of Co, the spin-down current is slightly higher than the spin-up current due to the larger value of the spin-down transmission at the Fermi level. The opposite happens for Ni due to the larger value of the spin-up transmission. Of special interest is the case of Fe. While at low bias most of the current contribution is from the spin-up component (as it is expected from Figs. 4 and 5), the spin-down current starts to rise faster at $V = 0.3$ V and surpasses the spin-up current around $V = 0.5$ V. This is due to the transmission peak associated to the d states which is initially located at 0.5 eV for the spin-down component and broadens and moves down in energy as the bias increases.

In order to gain insight into the spin-filtering properties of these systems, we plot in Fig. 7 the normalized spin current for each structure

$$\Delta I = \frac{I_\uparrow - I_\downarrow}{I_\uparrow + I_\downarrow}. \tag{7}$$

Notice that the value of this quantity is limited to the window $[-1,1]$. We find a very strong spin-filtering effect, up to 0.75, for the case of the FM Mo_2Fe_2 molecule at low bias. This effect disappears, however, as we increase the voltage. Also, there is a moderate spin-filtering effect for the AFM Mo_2Fe_2 and Mo_2Co_2 nanobridges at moderate voltages.

By comparing the AFM and FM cases it is also possible to determine whether magnetoresistive effects exist as a function of the bias voltage. Figure 8 shows the magnetoresistive properties of each nanobridge, quantified in terms of the normalized current difference between the AFM and FM configurations, divided by their sum:

$$\Delta I' = \frac{I_{\mathrm{AFM}} - I_{\mathrm{FM}}}{I_{\mathrm{AFM}} + I_{\mathrm{FM}}}. \tag{8}$$

Notice that this quantity is also limited to the window $[-1,1]$. Note that only the Fe nanobridge presents a small magnetoresistive effect at low bias, but it quickly disappears when the bias is increased. This suggest that these systems would only be useful for magnetoresistive applications in the case of $X = \mathrm{Fe}$ at low biases. By also including the spin-filtering effect, i.e., by calculating the magnetoresistance as a function of the spin component, we can see that the magnetoresistance is much bigger in all cases although it decreases steeply at large biases. These results show that the behavior of the AFM and FM spin arrangements is very similar at large biases, which implies that large voltages tend to destroy the magnetotransport response of the system.

V. CONCLUSIONS

We have studied the structural, electronic, and transport properties of magnetic nanoclusters with formula Mo_2X_2, where $X = \mathrm{Fe}$, Co, Ni. We have found that linear atomic arrangements, where the Mo atoms form a dimer, which is sandwiched by an X atom at each side, are the most stable nanostructures, with other possible two- or three-dimensional structures lying more than 0.1 eV higher in energy. This interesting feature renders these as inorganic alternatives to the more conventional organic molecular electronics devices. We have also found that the transition-metal atoms prefer to be antiferromagnetically coupled and have a magnetic moment that decreases from Fe to Ni.

We have analyzed the density of states of the ferromagnetic and antiferromagnetic configurations of the linear nanostructures both in isolation as well as coupled to two (001) gold electrodes. We have found that Fe- and Co-based clusters have a clear gap around the Fermi level which closes when the molecule is coupled to gold.

Finally we have studied the transport properties of the linear nanostructures coupled to the gold electrodes for both FM and

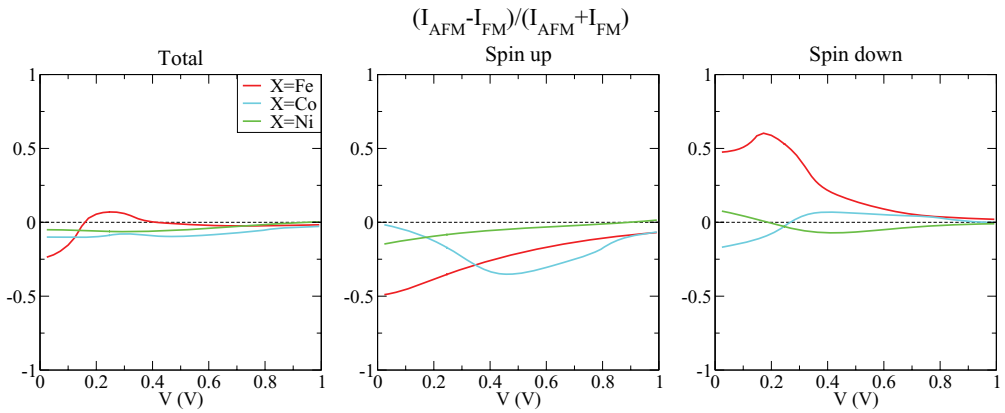

FIG. 8. (Color online) The magnetoresistive properties of the different Mo_2X_2 molecular junctions estimated from $\Delta I'$.

AFM spin arrangements. We have found that both spin-up and spin-down channels in the antiferromagnetic configuration give the same current and transmission at low bias voltages but start to differ at high biases; however, the current and transmission for the ferromagnetic cases are already different at zero bias. We have also calculated the difference between the currents in the ferromagnetic and the antiferromagnetic configurations to search for possible magnetoresistive effects and found that these are non-negligible only at low voltages.

These results indicate that the Fe-based nanobridges analyzed here could be used as inorganic nanospintronic devices. Spin-filtering and magnetoresistance effects are expected to appear in these and similar systems at low voltages.

ACKNOWLEDGMENTS

This work was supported by the Spanish Ministry of Science and Innovation (Projects No. FIS2011-22957 and No. FIS2009-07081), and by Junta de Castilla y León (Project No. VA104A11-2). VMGS thanks the Spanish Ministerio de Ciencia e Innovación for the support of a Ramón y Cajal Fellowship (RYC-2010-06053). AGF thanks the Spanish Ministry of Science and Innovation for an FPU grant.

[1] V. M. García-Suárez and C. J. Lambert, Phys. Rev. B **78**, 235412 (2008).
[2] A. Nitzan and M. A. Ratner, Science **300**, 1384 (2003).
[3] S. J. van der Molen and P. Liljeroth, J. Phys.: Condens. Matter **22**, 133001 (2010).
[4] C. Joachim and J. K. Gimzewski, Chem. Phys. Lett. **265**, 353 (1997).
[5] P. G. Piva, G. A. DiLabio, J. L. Pitters, J. Zikovsky, M. Rezeq, S. Dogel, W. A. Hofer, and R. A. Wolkow, Nature (London) **435**, 658 (2005).
[6] C. P. Collier, G. Mattersteig, E. W. Wong, Y. Luo, K. Beverly, J. Sampaio, F. M. Raymo, J. F. Stoddart, and J. R. Heath, Science **289**, 1172 (2000).
[7] B. L. Feringa, *Molecular Switches* (Wiley-VCH, Weinheim, 2001).
[8] Z. J. Donhauser, B. A. Mantooth, K. F. Kelly, L. A. Bumm, J. D. Monnell, J. J. Stapelton, D. W. Prince Jr., A. M. Rawlett, D. L. Allara, J. M. Tour, and P. S. Weiss, Science **292**, 2303 (2001).
[9] A. Mishchenko, D. Vonlanthen, V. Meded, M. Bürkle, C. Li, I. V. Pobelov, A. Bagrets, J. K. Viljas, F. Pauly, F. Evers, M. Mayor, and T. Wandlowski, Nano Lett. **10**, 156 (2010).
[10] An extensive review on molecular switches can be found in Ref. 3.
[11] E. G. Emberly and G. Kirczenow, Phys. Rev. Lett. **91**, 188301 (2003).
[12] Y.-H. Kim, S. S. Jang, Y. H. Jang, and W. A. Goddard III, Phys. Rev. Lett. **94**, 156801 (2005).
[13] R. Liu, S.-H. Ke, H. U. Baranger, and W. Yang, Nano Lett. **5**, 1959 (2005).
[14] L. Bogani and W. Wernsdorfer, Nat. Mater. **7**, 179 (2008).
[15] J. Ferrer and V. M. García-Suárez, J. Mater. Chem. **19**, 1696 (2009).
[16] S. Barraza-López, K. Park, V. M. García-Suárez, and J. Ferrer, J. Appl. Phys. **105**, 07E309 (2009).
[17] S. Barraza-López, K. Park, V. M. García-Suárez, and J. Ferrer, Phys. Rev. Lett. **102**, 246801 (2009).
[18] A. García-Fuente, A. Vega, F. Aguilera-Granja, and L. J. Gallego, Phys. Rev. B **79**, 184403 (2009).
[19] F. Aguilera-Granja, A. Vega, and L. J. Gallego, Nanotechnology **19**, 145704 (2008).
[20] T. He, Y. Gao, F. Zeng, and F. Pan, J. Phys. D **37**, 1 (2004).
[21] M. N. Baibich, J. M. Broto, A. Fert, F. Nguyen Van Dau, F. Petroff, P. Etienne, G. Greuzet, A. Friedrich, and J. Chazelas, Phys. Rev. Lett. **61**, 2572 (1988).
[22] G. Binasch, P. Grünberg, F. Saurenbach, and W. Zinn, Phys. Rev. B **39**, 4828 (1989).
[23] S. Datta, *Electronic Transport in Mesoscopic Systems* (Cambridge University Press, Cambridge, UK, 1995).
[24] A. R. Rocha, V. M. García-Suárez, S. W. Bailey, C. J. Lambert, J. Ferrer, and S. Sanvito, Phys. Rev. B **73**, 085414 (2006).
[25] A. R. Rocha, V. M. García-Suárez, S. W. Bailey, C. J. Lambert, J. Ferrer, and S. Sanvito, Nat. Mater. **4**, 335 (2005).
[26] W. Kohn and L. J. Sham, Phys. Rev. **140**, A1133 (1965).
[27] J. M. Soler, E. Artacho, J. D. Gale, A. García, J. Junquera, P. Ordejón, and D. Sánchez-Portal, J. Phys.: Condens. Matter **14**, 2745 (2002).
[28] N. Troullier and J. L. Martins, Phys. Rev. B **43**, 1993 (1991).
[29] L. Kleinman and D. M. Bylander, Phys. Rev. Lett. **48**, 1425 (1982).
[30] J. P. Perdew, K. Burke, and M. Ernzerhof, Phys. Rev. Lett. **77**, 3865 (1996).
[31] We note that, as in most DFT simulations, GGA tends to underestimate the gap and can give spurious results, especially in systems with transition-metal atoms and large charge transfer. This can be corrected by adding a U term (GGA + U) [A. R. Rocha, T. Archer, and S. Sanvito, Phys. Rev. B **76**, 054435 (2007)]. However, if there are no sharp features in the transmission at the Fermi level the inclusion of the U term reduces to simply opening the highest occupied molecular orbital (HOMO)-LUMO gap, which decreases the value of the current. We therefore expect the shape of the $I-V$ characteristics to be very similar. A note of caution should be added, however, because the U term could affect the magnetoresistance and rectification ratios.
[32] The DFT calculations are performed at zero temperature, which means temperature effects such as phonons and atomic displacements are not taken into account. The only temperature effect which is included is the electronic contribution that appears in the Fermi distribution function. This factor does not affect the results for T below 300 K. The effect of phonons is usually small but other thermic effects can lead to more pronounced changes. These mainly include conformation changes in the molecular backbone, which in this case are not important due to the linear shape of the most stable molecular configuration, and changes in the coupling configuration, which produce different conductance values that are seen as different peaks in the histograms. These peaks are less important and frequent than that which corresponds to the most stable configuration.
[33] Since the system is very small it is therefore sensitive to external parameters, as it happens in all molecular electronics experiments, where the presence of many possible configurations makes necessary the use of histograms. A study that takes into account all possible factors is beyond the scope of the present paper. However, in general such a study is not strictly necessary because the most probable conductance configuration, that which corresponds to just the peak value in the histogram, is expected to be the most relevant.